

The Long-term Period Changes of the Cepheid Variable SV Monocerotis

Pradip Karmakar

Department of Mathematics, Madhyamgram High School (H.S.), Madhyamgram, Sodepur Road, Kolkata 700129, India; pradipkarmakar39@gmail.com

Gerard Samolyk

P.O. Box 20677, Greenfield, WI 53220; gsamolyk@wi.rr.com

Received December 15, 2020; revised August 17, October 14, 2021; accepted October 20, 2021,

Abstract We present the long-term period changes of the Cepheid variable SV Mon, as determined by a parabolic fit to archived observations made from 1911 through mid-2021. We found that its period is increasing at a rate of 4.1 s/yr, showing a long-term evolutionary trend.

1. Introduction

The pulsation period changes of Cepheids have the potential to provide information about their evolutionary trend through the instability strip (Neilson *et al.* 2016). The O–C diagram of a star that has a constant but slow rate of period change is well represented by a parabola. For a Cepheid, such a quadratic fit allows the rate of observed period change to be compared with the theoretical rate of period change. Experience has shown that when the time interval spanned by the O–C diagram approaches a century, the observations are sufficient to reveal evolutionary changes of a Cepheid (Turner *et al.* 2006). Therefore, when the variability of Cepheid periods is studied, the longest possible time interval should be covered by observations.

Observations of SV Mon under the AAVSO Classical Cepheid Program headed by Thomas A. Cragg (Cragg 1972) began in the period JD 2440000–2441000 (23 May 1968–17 February 1971).

The primary purpose of that program was to investigate the slow period changes of the classical Cepheids of period greater than 10.0 days. In this first study 134 observations of SV Mon were obtained which could be well described by a period of 15.2321 days. The value of O–C was nearly zero. The visual magnitude range was 8.5–9.

In their second study, they observed long-period classical Cepheids for the next 1,000 days (JD 2441000–2442000, 17 February 1971–13 November 1973) (Cragg 1975). In this series Landis, one of the observers of this program, collected mostly photoelectric measurements and k-factors were used to adjust individual observers' measurements to the mean light curve. Little meaningful change had been observed in O–C value. In this session, the time of maximum light's date in JD (M) minus time of minimum light's date in JD (m) i.e. M–m, was 0.33 P (P = 15.2 days (0.35P according to GCVS, Kukarkin *et al.* (1969))). In this session a little hip in the light curve of SV Mon was observed.

In their third phase study, JD 2442000–2443000 (13 November 1973–09 August 1976) (Cragg 1983), they observed SV Mon and obtained 147 observations of it. The O–C value was +1.5 days. M–m was 6 days = 0.39 P (0.35 P in GCVS).

In an another study of period change of this Cepheid, Szabados (1981) considered the visual (vis), photographic (pg),

and photoelectric (pe) data sets and showed that there was no significant change in period. In this study the O–C residuals were calculated using the formula:

$$C = 2443794.338 + 15.232780 d * E \quad (1)$$

In his next study, Szabados (1991) found that the new pulsation period of SV Mon, determined only from photoelectric data, was somewhat shorter than that determined in his previous study (Szabados 1981). In the 1991 study the O–C residuals were calculated using the elements:

$$C = 2443794.249 (\pm 0.019) + 15.232582 d (\pm 0.000073) * E \quad (2)$$

In the current paper we study the behavior of the pulsations of the low-amplitude Cepheid SV Mon; the period of its brightness variation (P) used is 15.23278 days, given in the AAVSO's International Variable Star Index (VSX; Watson *et al.* 2014).

2. Techniques and observational data

For this new period change study of SV Mon, initially we considered visual observational data downloaded from the AAVSO International Database (Kafka 2021) from 1967 to mid-2020, i.e. for a time span of nearly 50 years; we excluded the photoelectric measurements observed by Landis in JD 2441000–2442000 as these observational records are not available in the AAVSO International Database.

Next, we considered the V filter (PEP and CCD) AAVSO magnitudes (1954–mid 2021; Kafka 2021) and ASAS (2002–2009; Pojmański 1997).

We also have considered the visual, photographic, and photoelectric data sets collected from Szabados' two papers (1981, 1991).

We divided the total data set yearly. Then we needed to determine the time of maximum light (TOMax) of SV Mon. For this purpose we used the AAVSO's VSTAR package (Benn 2012, 2013). To determine the O–C values, we considered $T_0 = 2443794.338$ and the initial period, $P = 15.23278$ days. Both of these values were obtained from VSX.

3. Period change analysis of SV Mon

Figures 1 and 2 show the phased visual and non-visual (CCD) light curves of SV Mon. Figure 3 shows an O–C diagram for SV Mon, using visual and non-visual photometric data, calculated according to the ephemeris (light elements) $T_{\max} = 2443794.338 + 15.23278E$, where T_{\max} is the predicted time of maximum light and E is the number of elapsed cycles.

Table 1 lists the times of maxima (JD), cycles, O–C residuals, and type of observation. We subtracted 2400000 from the Julian Date in order to reduce the number of significant digits and so increase the accuracy of the calculation.

Visual inspection shows that the actual period is longer than the VSX period. We used the data set from 1911 to mid-2021 and constructed an O–C diagram, then added a parabolic fitted curve to the O–C diagram (Figure 3).

It is clear from Figure 3 that the period is increasing.

$$JD_{\max} = a + bE + cE^2 \quad (3)$$

We fit Equation (3) to the Times of maximum (JD) and E (Cycle) given in Table 1, and derived the following ephemeris (light elements) (Equation 4):

$$JD_{\max} = 9.9 \times 10^{-7} (\pm 1.4 \times 10^{-7}) E^2 + 15.234 (\pm 0.00011) E + 2443795 (\pm 0.091) \quad (4)$$

The period rate of increase since 1911 can be deduced by Equation (5):

$$\frac{dP}{dt} = 2 \times (9.9 \times 10^{-7}) \times \left(\frac{1}{15.234} \right) \times (86400) \times 365.25 = 4.1 \text{ s/yr} \quad (5)$$

$$O-C = a + bE + cE^2 \quad (6)$$

We fit Equation (6) to the O–C and E (Cycle) values in Table 1, and derived the following fitted parabola:

$$O-C = 9.94 \times 10^{-7} (\pm 1.4 \times 10^{-7}) E^2 + 0.0012 (\pm 0.00011) E + 0.684 (\pm 0.091) \quad (7)$$

From Equation 7, it is clear that the value of c (9.94×10^{-7}) is greater than 0 (zero), so the fitted parabola is in the upward direction. Hence we can suggest that the period of SV Mon is increasing.

4. Conclusions

As presented in section 3, the photometric observations of SV Mon covering about 111 years (1911–mid-2021) indicate the increasing nature of its period, as demonstrated by the parabolic interpretation of the O–C diagram in Figure 3. From our analysis we conclude that SV Mon has a trend of period increase of 4.1 s/yr for the years 1911 to mid-2021.

5. Acknowledgements

We thank the AAVSO and ASAS for the use of the data from their archives and L. Szabados for his two papers (Szabados,

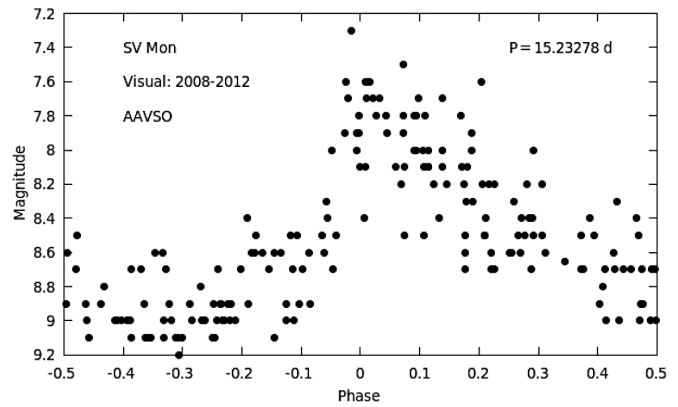


Figure 1. The visual light curve of SV Mon.

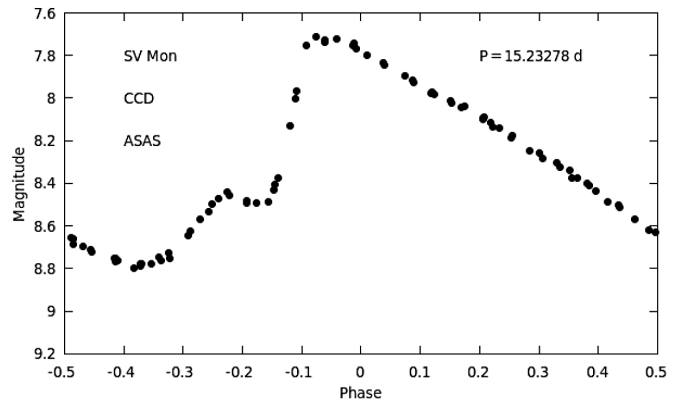


Figure 2. The CCD V-band light curve of SV Mon.

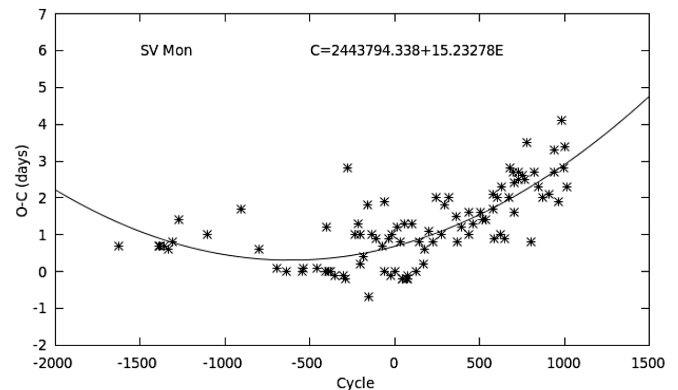


Figure 3. Period change of SV Mon. The O–C versus Cycle diagram of SV Mon, drawn from the TOMax and epochs (cycles) listed in Table 1. The solid curve is a parabolic fit to the data. All O–C residuals (shown as x) were computed with the ephemeris $C = 2443794.338 + 15.23278E$ (via VSX, from Szabados 1981).

1981, 1991), from where we have collected all the data sets of SV Mon for our paper. We also thank the referee for their help and advice in the improvement of our paper. We are very grateful to Kevin B. Alton and David Benn for their help about using VSTAR to determine the time of maximum light of SV Mon. We are also grateful to Horace A. Smith for his fruitful suggestions for the improvement of our paper.

Table 1. O–C residuals of the Times of Maxima (TOMax) in Julian days (JD) for SV Mon from 1911 to mid-2021 of visual (AAVSO International Database (Kafka 2021); Szabados (1981)) and non-visual (AAVSO, ASAS (Pojmański 1997), and Szabados (1981, 1991)) photometry.

TOMax (JD2400000+)	Cycle (E)	O–C	Type	TOMax (JD2400000+)	Cycle (E)	O–C	Type
19041.759	–1625	0.7	pg	45683.183	124	0	pe
22621.464	–1390	0.7	vis	46049.58	148	0.8	vis
22728.089	–1383	0.7	vis	46414.6	172	0.2	vis
23047.978	–1362	0.7	vis	46521.61	179	0.6	vis
23459.184	–1335	0.6	vis	46872.5	202	1.1	vis
23809.69	–1312	0.8	vis	47222.5	225	0.8	vis
24419.65	–1272	1.4	vis	47543.6	246	2	vis
27008.827	–1102	1	vis	47999.54	276	1	vis
29964.707	–908	1.7	vis	48274.53	294	1.8	vis
31608.67	–800	0.6	vis	48655.56	319	2	vis
33192.42	–696	0.1	pg	49340.6	364	1.5	vis
34045.326	–640	0	pg	49385.6	367	0.8	vis
35477.219	–546	0	pe	49751.58	391	1.2	vis
35538.224	–542	0.1	pg	50421.63	435	1	vis
36848.276	–456	0.1	pg	50452.68	437	1.6	vis
37564.109	–409	0	pe	50863.63	464	1.3	vis
37656.731	–403	1.2	ccd	51488.46	505	1.6	vis
37899.291	–387	0	pe	51640.64	515	1.4	vis
38097.263	–374	0	pg	51960.56	536	1.4	vis
38386.627	–355	–0.1	pg	52615.8	579	1.7	vis
39209.191	–301	–0.1	pe	52646.697	581	2.1	ccd
39346.203	–292	–0.2	pe	52706.38	585	0.9	vis
39577.7	–277	2.8	vis	53042.62	607	2	ccd
40215.6	–235	1	vis	53315.8	625	1	vis
40474.9	–218	1.3	vis	53408.564	631	2.3	ccd
40672.6	–205	1	vis	53711.8	651	0.9	vis
40732.705	–201	0.2	pe	54093.66	676	2	vis
40976.7	–185	0.4	vis	54170.65	681	2.8	vis
41343.64	–161	1.8	vis	54444.737	699	2.7	ccd
41493.5	–151	–0.7	vis	54520.5972	704	2.4	ccd
41784.6	–132	1	vis	54565.48	707	1.6	vis
42119.63	–110	0.9	vis	54886.29	728	2.5	vis
42728.74	–70	0.7	vis	54947.48	732	2.7	ccd
42836.54	–63	1.9	vis	55297.65828	755	2.6	ccd
42865.108	–61	0	pe	55510.82	769	2.5	vis
43231.63	–37	0.9	vis	55664.15	779	3.5	vis
43489.586	–20	–0.1	pe	55996.56	801	0.8	vis
43551.57	–16	1	vis	56333.59	823	2.7	vis
43794.342	0	0	pe	56668.35	845	2.3	vis
43993.59	13	1.2	vis	57094.56	873	2	vis
44282.56	32	0.8	vis	57658.29	910	2.1	vis
44449.175	43	–0.2	pe	58101.25	939	3.3	vis
44525.339	48	–0.2	pe	58131.04	941	2.7	vis
44648.64	56	1.3	vis	58541.6	968	1.9	vis
44890.941	72	–0.2	pe	58802.74746	985	4.1	ccd
44967.09	77	–0.2	pe	58938.55	994	2.8	vis
44997.62	79	–0.1	vis	59121.88933	1006	3.4	ccd
45364.58	103	1.3	vis	59303.59368	1018	2.3	ccd

References

- Benn, D. 2012, *J. Amer. Assoc. Var. Star Obs.*, **40**, 852.
- Benn, D. 2013, VSTAR data analysis software (<https://www.aavso.org/vstar-overview>).
- Cragg, T. A. 1972, *J. Amer. Assoc. Var. Star Obs.*, **1**, 9.
- Cragg, T. A. 1975, *J. Amer. Assoc. Var. Star Obs.*, **4**, 68.
- Cragg, T. A. 1983, *J. Amer. Assoc. Var. Star Obs.*, **12**, 20.
- Kafka, S. 2021, Observations from the AAVSO International Database (<https://www.aavso.org/data-download>).
- Kukarkin, B. V., et al. 1969, *General Catalogue of Variable Stars, Volume 1*, Moscow.
- Neilson, H. R., Percy, J. R., and Smith, H. A. 2016, *J. Amer. Assoc. Var. Star Obs.*, **44**, 179.
- Pojmański, G. 1997, *Acta Astron.*, **47**, 467 (<http://www.astro.uw.edu.pl/asas>).
- Szabados, L. 1981, *Commun. Konkoly Obs.*, **77**, 1.
- Szabados, L. 1991, *Commun. Konkoly Obs.*, **96**, 123.
- Turner, D. G., Abdel-Sabour Abdel-Latif, M., and Berdnikov, L. N. 2006, *Publ. Astron. Soc. Pacific*, **118**, 410.
- Watson, C., Henden, A. A., and Price, C. A. 2014, AAVSO International Variable Star Index VSX (Watson+, 2006–2014; <https://www.aavso.org/vsx>).